Hydrogen-bonded siloxane liquid crystals for hybrid nanomaterials

Hydrogen-Bonded Siloxane Liquid Crystals for Hybrid Nanomaterials

Koen Nickmans,[a] Sjoerd O. Jansma,[a] Daniela Hey,[a] Gangamallaiah Velpula,[b] Joan Teyssandier,[b] Steven De Feyter,*[b] and Albert P. H. J. Schenning*[a]

[a]Laboratory of Stimuli-responsive Functional materials and Devices (SFD), Department Chemical Engineering & Chemistry, Eindhoven University of Technology, P.O. Box 513, NL-5600 MB Eindhoven, The Netherlands, e-mail: a.p.h.j.schenning@tue.nl

[b]Division of Molecular Imaging and Photonics, Department of Chemistry, KU Leuven, Celestijnenlaan 200F, BE-3001 Leuven, Belgium, e-mail: steven.defeyter@kuleuven.be

Dedicated to *François Diederich* on the occasion of his retirement.

The self-assembly of molecular inorganic/organic hybrid building blocks into ordered hierarchical nanomaterials with a tunable morphology is an enormous challenge. Here, we describe the synthesis and characterization of a novel liquid crystalline hydrogen-bonding hepta(dimethylsiloxane) azobenzene carboxylic acid dimer. This inorganic/organic hybrid dimer forms sub-5 nm lamellar features in the bulk and at the liquid solid interface. When mixed with a complementary hydrogen-bonding disk-shaped small molecule, a columnar hexagonal phase is formed. When adding a block copolymer containing hydrogen bond-accepting moieties, a hierarchical nanostructured material is obtained with a hexagonal columnar arrangement perpendicular to lamellae super structure. Our supramolecular approach shows that hierarchical hybrid nanomaterials can be fabricated with controlled properties which is appealing for applications such as nanoporous materials, organic electronics, and nanolithography.

Keywords: hierarchical structures, hydrogen bonds, liquid crystals, nanomaterials, siloxane molecules, supramolecular chemistry.

Introduction

Self-assembly is an appealing bottom-up method for fabricating functional nanomaterials. Nanostructured materials are interesting for applications such organic electronics, nanoporous membranes, and nanolithography.[1 – 3] The self-assembly of block copolymers (BCPs) through microphase separation of incompatible blocks is an attractive method for preparing such nanomaterials.[4][5] Typically, BCPs form nanostructures with features in the 10 – 100 nm regime.[6] Over the past few decades, the self-assembly of liquid crystals (LCs) which can be considered as a state of matter between the liquid and solid phases, has proven to be a useful tool in the development of well-defined sub-5 nm structured materials.[1][7 – 14] Depending on the chemical structure and shape, different morphologies, *i.e.* columnar, lamellar, or bicontinuous mesophases, can be formed.[15] The self-assembly of these materials on the nanometer scale can be manipulated using alignment layers, electric or magnetic fields, shear forces, or light,[16][17] resulting in materials with a monolithic structure on macroscopic length scales produced with large scale and low cost processes. The generation of such ordered nanostructured materials is comparatively straightforward, in contrast to the self-assembly of block copolymers.[1][18]

For the construction of nanostructured materials with sub-5 nm patterns, hybrid organic/inorganic small molecules such as those based on polyhedral oligomeric silsesquioxane[19][20] or oligo(dimethylsiloxane)[21 – 25] (ODMS) are attractive. The chemical immiscibility of the organic and inorganic segments leads to phase separation into highly ordered nanostructures[26] and a high etch contrast between organic and inorganic parts.[1] For example, these materials could be used to fabricate inorganic nanostructure arrays with sub-5 nm features by etching. To date, however, the self-assembly of liquid crystalline hybrid organic/inorganic molecules has hardly been explored. We previously reported a series of ODMS liquid crystals (LCs) that formed large-area ordered sub-5 nm structures by graphoepitaxy,[21] and photoalignment.[17] The morphology of the structures could be tuned by length of the ODMS tail.[21] We now report on the synthesis and self-assembly of a novel liquid

DOI: 10.1002/hlca.201800130 *Helv. Chim. Acta* **2018**, *101*, e1800130

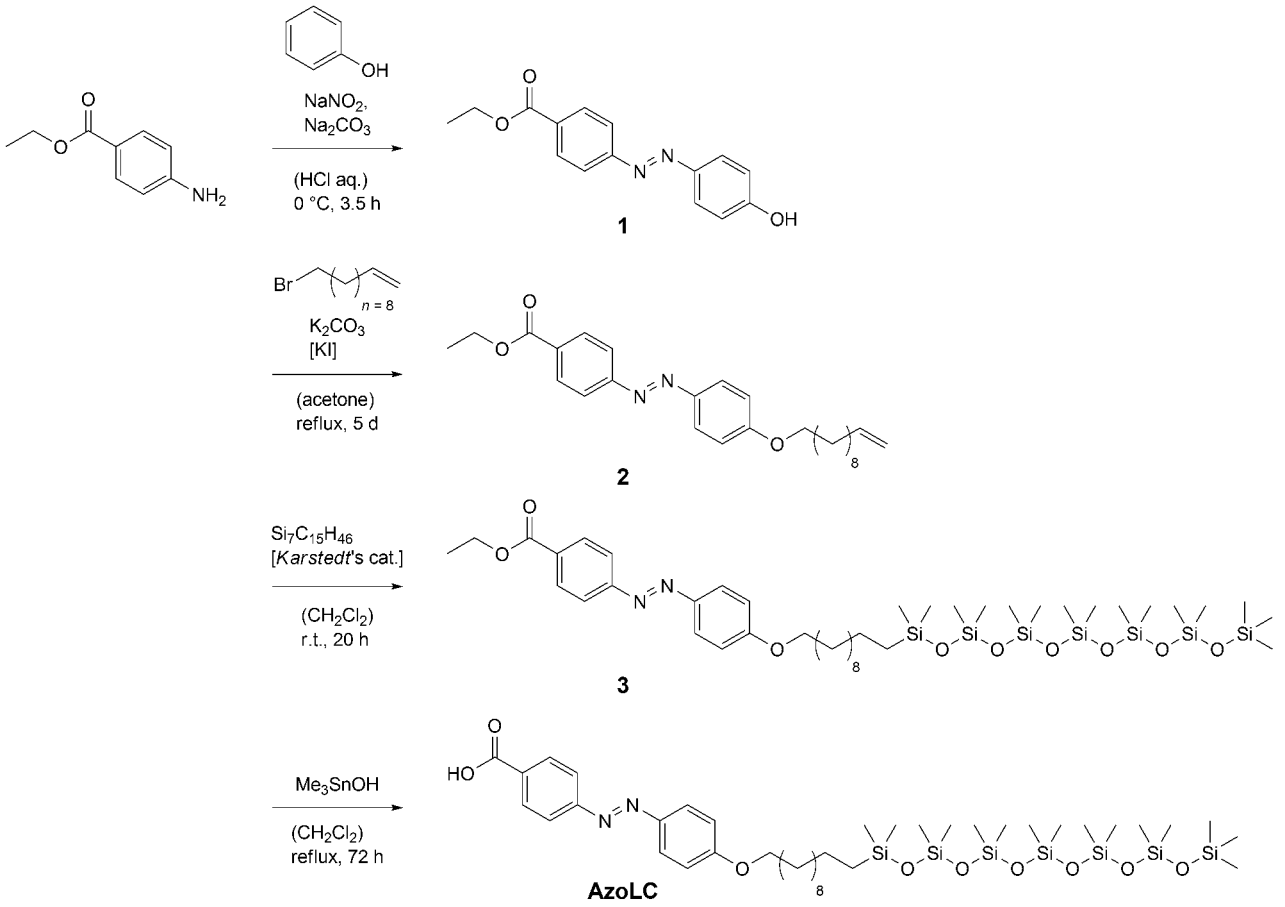

Scheme 1. Synthetic scheme for the preparation of the hepta(dimethylsiloxane) azobenzene carboxylic acid **AzoLC**.

crystalline hepta(dimethylsiloxane) azobenzene carboxylic acid (**AzoLC**, *Scheme 1*) of which the nanostructured morphology can be tuned by complementary hydrogen bonding with disk-shaped small molecules. Furthermore, hierarchical supramolecular materials can be obtained by mixing **AzoLC** with a block copolymer containing a hydrogen bond accepting block.

Results and Discussion

The synthetic scheme for the preparation of the hydrogen bonded hepta(dimethylsiloxane) azobenzene carboxylic acid **AzoLC** is shown in *Scheme 1*. A diazo coupling reaction was performed starting from ethyl 4-aminobenzoate and phenol to yield intermediate **1**. The resulting hydroxyl-functionalized azobenzene **1** was reacted with alkyl bromide 11-bromoundec-1-ene in a *Williamson* ether synthesis to form intermediate **2**. The synthesis of heptasiloxane monohydride which was subsequently coupled to **2** using *Karstedt*'s catalyst to yield intermediate **3** has been published before[27]. Finally, intermediate **3** was deprotected using trimethyltin hydroxide to produce **AzoLC**.[28] Mild base trimethyltin hydroxide was preferred over sodium hydroxide, since the latter resulted in decomposition of the ODMS. **AzoLC** was purified and fully characterized. The synthetic procedures and characterization are provided in the *Experimental Section*.

According to polarized optical microscopy (POM) and differential scanning calorimetry, **AzoLC** exhibits various LC mesophases with corresponding birefringent multi-domain textures (*Figure S1*, see *Supporting Material*). The texture at room-temperature (*Figure 1,c*) corresponds to those previously observed for siloxane LCs[21] and indicate the formation of a smectic phase. Infra-red (IR) spectroscopy (*Figure S2*) shows a C=O stretching vibration at 1683 cm^{-1} indicative for the formation of hydrogen-bonded carboxylic acids (*Figure 1,a*). X-Ray diffraction at room temperature reveals highly ordered lamellar features (clearly visible up to 5^{th} order) with a lattice spacing of a = 5.04 nm (*Figure 1,b*). Since this value is approximately double the molecular length, it is assumed that hydrogen-bonded dimers are formed. In the wide angle region (q > 10 nm^{-1}), some higher-order scatterings are

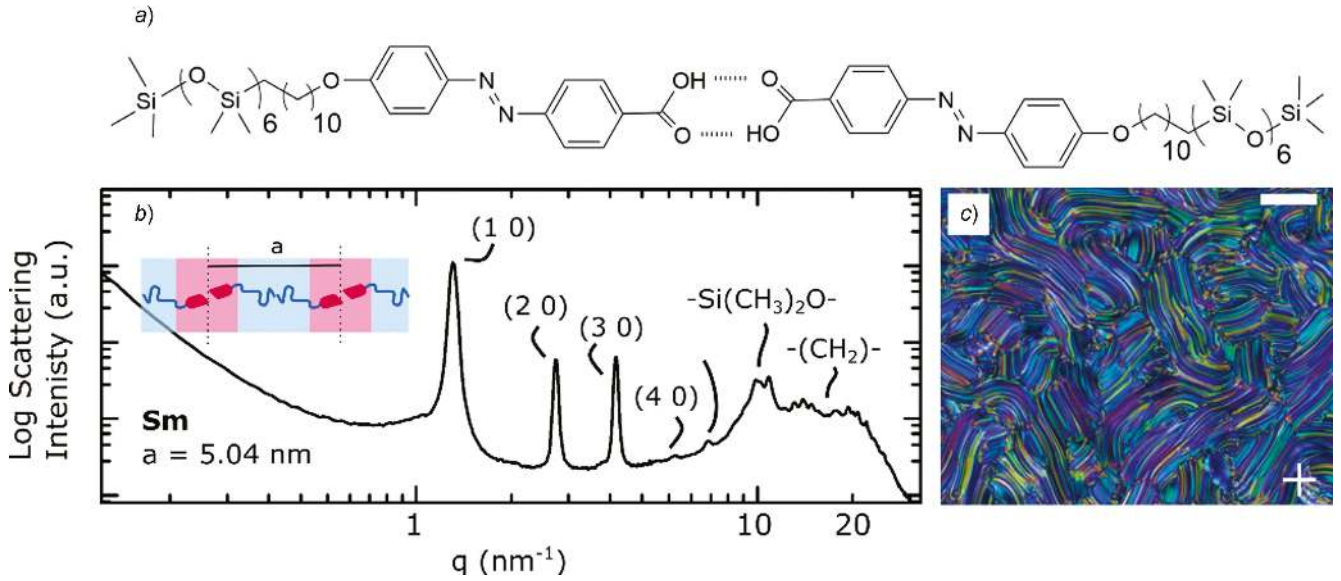

Figure 1. *a*) Chemical structure of the hydrogen bonded hepta(dimethylsiloxane) azobenzene carboxylic acid **AzoLC** dimer. *b*) X-Ray scattering data of **AzoLC** obtained at room temperature with the assigned lattice constant and *Miller* indices. *c*) Polarized optical microscopy image obtained at room temperature under crossed polarizers. The polarizer axes are shown in the image. Scale bar: 100 μm.

observed in addition to the broad scatterings corresponding to the mean distance between siloxane-siloxane (q = 9 nm^{-1} (d = 0.70 nm)) and aliphatic and aromatic parts of the molecule (q = 13.4 nm^{-1} (d = 0.45 nm)).[21] The additional reflections are likely due to partial crystallization of the organic part of the molecule, which may act as a driving force for the high order.[24] Nevertheless, the typical textures observed in polarized optical microscopy indicate that the material is liquid crystalline.

The self-assembly of **AzoLC** was further investigated at the liquid/solid interface using scanning tunneling microscopy (STM) under ambient conditions. This scanning probe microscopy technique is a powerful means to reveal the structure of self-assembled molecules on conductive surfaces.[29 – 31] Panels (*a*) and (*b*) of *Figure 2* show large- and small-scale STM images of **AzoLC** at the 1-phenyloctane (1-PO)/highly oriented pyrolytic graphite (HOPG) interface, respectively. **AzoLC** readily forms stable self-assembled molecular networks, most likely monolayers, at this interface. The network exhibits a lamellar organization with alternating bright and dark rows. Smaller scale molecular resolution STM images such as the one shown in *Figure 2,b* reveal that the bright features arise from rows of rod shaped structures, likely corresponding to the aromatic parts of the molecule.[32] The alkyl chains could not be resolved, possibly in view of their mobility on the surface on the time scale of STM measurement. The unit cell parameters are: a = 3.7 ± 0.1 nm, b = 1.4 ± 0.1 nm, and α = 88.0 ± 1.0°, which corresponds closely to those previously observed for alkylated azobenzene carboxylic acids.[32] We therefore propose in *Figure 2,c* a tentative model of the self-assembled network consisting of a combination of hydrogen-bonded **AzoLC** dimers and alkyl chains present in adjacent rows. The siloxane chains cannot fit within the unit cell and are assumed not to be adsorbed on the graphite surface, but rather back-folded in the supernatant solution phase.[33]

Next, the self-assembly of **AzoLC** was investigated in the presence of a complementary hydrogen-bonding disc-like small molecule **MeTBIB** (1,3,4-tris(6-methyl-1*H*-benzo[*d*]imidazol-2-yl)benzene). When **MeTBIB** is mixed with **AzoLC** in a 1:3 ratio, the POM shows a texture indicative for a columnar phase (*Figure 3,b*). The IR spectrum displays a shift of the C=O stretching vibration from 1683 cm^{-1} to 1675 cm^{-1}, while a peak around 3260 cm^{-1} is present which can be assigned to NH vibrations.[34] X-Ray analysis confirms the formation of columnar hexagonal phase with a periodicity of 6.66 nm (*Figure 3,a,c*). This periodicity corresponds well with two times the length of **AzoLC** and the diameter of **MeTBIB**. Compared to the hydrogen-bonded dimer, crystallization is suppressed. However, a new peak is present in the wide-angle region at approximately (q = 19.0 nm^{-1} (d = 0.33 nm)) which likely corresponds to the inter-disc distance.[34] All these results reveal the formation of a hydrogen-bonded complex between **MeTBIB** and **AzoLC**

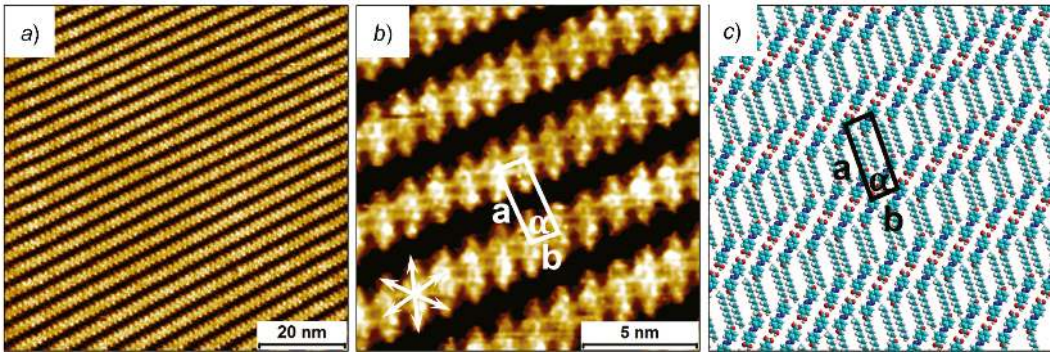

Figure 2. **AzoLC** at the 1-PO/HOPG interface. *a*) Large-scale STM image of the self-assembled monolayer (C_{AzoLC} = 1.0 × 10^{-4} M). *b*) Small-scale STM image of the self-assembled monolayer (C_{AzoLC} = 1.0 × 10^{-4} M). The imaging parameters are: I_{set} = 100 pA, V_{bias} = 900 mV. The graphite symmetry axes are shown in the lower left corner by white arrows. *c*) Tentative molecular model showing the arrangement of **AzoLC** molecules in the SAMN. The siloxane chains are omitted for the sake of clarity. The unit cell is overlaid on the STM image and molecular model. The unit cell parameters are: a = 3.7 ± 0.1 nm, b = 1.4 ± 0.1 nm, and α = 88.0 ± 1.0°.

forming a columnar supramolecular structure with the columns packed in a hexagonal lattice (*Figure 3,c*).

In order to fabricate hierarchical nanomaterials, **AzoLC** was mixed with a poly(styrene)-b-poly(4-vinylpyridine) (PS-b-PVP) block-copolymer in a 0.3:1 ratio. After mixing, the POM shows a grainy birefringent texture (*Figure 3,e*), which is consistent with the formation of a homogenous blend. The IR spectrum displays a shift of the C=O stretching vibration from 1683 cm^{-1} to 1695 cm^{-1} indicating that the carbonyl groups are no longer involved in hydrogen bonding once the acid–pyridine hydrogen bond is formed.[23][35] The PS-b-P4V-**AzoLC** mixture was further investigated by XRD. To capture the hierarchical multi-scale self-assembly, scattering data was obtained in small-angle and medium-angle configurations. A hexagonal columnar in a lamellar phase is observed with a lamellar spacing of d = 39.8 nm and a hexagonal periodicity of a = 6.1 nm (*Figure 3,d*). The layered distance of *ca.* 40 nm corresponds well with the BCP lattice spacing while the features with a periodicity of *ca.* 6 nm matches with the pyridine block-**AzoLC** phase. Most likely, the hexagonal arrangement is oriented perpendicular to lamellae structure similar as observed previously for hierarchical supramolecular block copolymer assemblies.[23][36][37]

Conclusions

A novel hydrogen bonding hepta(dimethylsiloxane) azobenzene carboxylic acid dimer has been prepared and fully characterized. The inorganic/organic hybrid dimers form a liquid crystalline smectic phase in the solid state and lamellar patterns at the liquid-solid interface. The morphology can be changed when mixed with a complementary hydrogen-bonding disk-shaped small molecule, and a columnar hexagonal phase is formed. Hierarchical nanomaterials having a hexagonal columnar arrangement perpendicular to lamellae super structure can be fabricated when adding a block copolymer containing hydrogen bond-accepting moieties. This supramolecular approach results in new hybrid nanomaterials with tuned ordered hierarchical structures. These findings are interesting for a variety of applications such organic electronics, nanoporous materials, and nanolithography. However, in order to utilize these materials, the alignment of these supramolecular structures should be explored. For example, the azobenzene-containing hierarchical materials reported here could be combined with photo-alignment processes in order to obtain oriented monodomain structures by exposure to linearly polarized light, or act as photo-switches (*Figure S3*).[17] The directed hierarchical self-assembly of block copolymers with small molecules could also be explored to create hybrid nanomaterials with well-defined hierarchical features.[23]

Experimental Section

Materials and Methods

Heptasiloxane monohydride was kindly synthesized by *Bas de Waal* and obtained from the group of *Meijer*. **MeTBIB** (2,2′,2″-benzene-1,2,4-triyltris(6-methyl-1*H*-benzimidazole)) was kindly synthesized by *Jody Lugger* and obtained from the group of *Sijbesma*. PS_{33k}-b-$P4VP_{8k}$ (f_{PS} ~0.8) (PDI = 1.06) block copolymer was purchased from *Polymer Source*. All solvents and standard chemicals were obtained from commercial sources and were used as received. Reactions with air- or moisture-sensitive reagents were performed under argon atmosphere with flame-dried glassware using standard *Schlenk* techniques. Nuclear magnetic

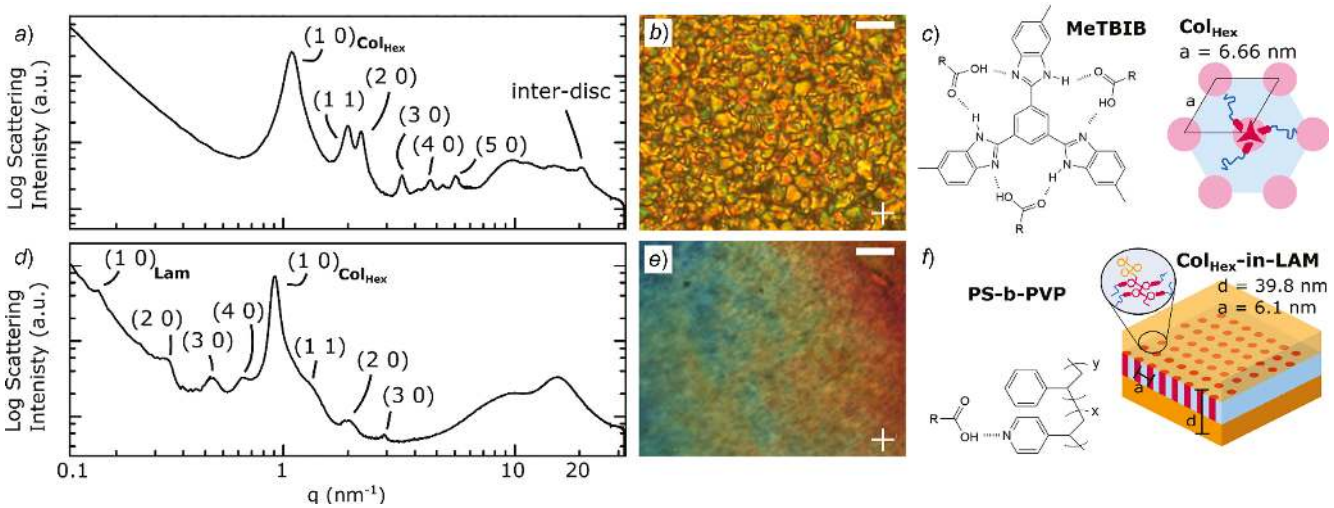

Figure 3. *a*) X-ray scattering data of **AzoLC** with **MeTBIB** (3:1) at room temperature with the assigned lattice constants and miller indices. *b*) Polarized optical microscopy image obtained at room temperature under crossed polarizers. The polarizer axes are shown in the image. Scale bar: 100 μm. *c*) Proposed supramolecular arrangement of the **AzoLC** with **MeTBIB** (3:1) in the solid state. *d*) X-Ray scattering data of **AzoLC** with poly(styrene)-b-poly(4-vinylpyridine) block-copolymer (3:1) at room temperature with the assigned lattice constants and *Miller* indices. *e*). Polarized optical microscopy image obtained at room temperature under crossed polarizers. The polarizer axes are shown in the image. Scale bar: 100 μm. *f*) Proposed supramolecular arrangement of the **AzoLC** with **MeTBIB** (3:1) in the solid state.

resonance spectra (NMR spectra) were measured on a *Varian Mercury 400Vx* and a *Bruker 400MR* NMR apparatus at 300 K. Chemical shifts are indicated as δ values in parts per million [ppm] and are reported relative to $CHCl_3$. Mass spectra were measured on a *Bruker ST-A2130* mass spectrometer with matrix-assisted laser desorption ionization and a time-of-flight analyzer (MALDI-TOF) using a 2 kHz laser. Depending on the measured substance, α-cyano-4-hydroxycinnamic acid (CHCA) or 2-[(2*E*)-3-(4-*tert*-butylphenyl)-2-methylprop-2-enylidene]malononitrile (DCTB) in tetrahydrofuran (THF) were applied as matrices. Substances were detected with a *Bruker Flash Detector*. Infrared spectra were measured on a *Bruker Optics Tensor 27* FT-IR spectrometer at room temperature applying Attenuated Total Reflectance (ATR) technique. The following abbreviations are used for labelling of the signals in the spectra: *w* = weak, *m* = middle, *s* = strong, br. = broad. Polarized optical microscopy (POM) was performed with crossed polarizers using a *Leica DM6000M* equipped with a *DFC420C* camera and a *Linkam THMS600* hot-stage for temperature control. For characterization of the LC textures, a small amount of LC material was placed between microscope slides, heated to the isotropic phase, and cooled (5 °C min^{-1}) to room temperature. Phase transition temperatures of the reactive mesogens were determined using a *TA Instrument Q1000* differential scanning calorimeter (DSC). Three to four miligrams of material was hermitically sealed in aluminum pans. The heating and cooling rate was 10 °C min^{-1}, and the second cooling curve was used to determine the transition temperatures.

XRD Measurements

X-Ray scattering measurements were performed on a *Ganesha* lab instrument equipped with a *GeniX-Cu* ultralow divergence source producing X-ray photons with a wavelength of 1.54 Å and a flux of 1×10^8 phs^{-1}. Scattering patterns were collected using a *Pilatus 300 K* silicon pixel detector. The beam center and the *q* range were calibrated using the diffraction peaks of silver behenate. The sample to detector distance was 91 mm for wide-angle measurements, and 441 mm for medium-angle measurements. The spectra were concatenated at $q = 5$ nm^{-1}.

STM Measurements

For STM imaging, a stock solution of **AzoLC** (1.0×10^{-3} M) was prepared by dissolving appropriate amount of solid in 1-phenyloctane (*Sigma–Aldrich*, ≥ 98%). The stock solution was diluted further to make concentration series. All STM experiments were performed at room temperature (21 – 23 °C) using a *PicoLE* (*Agilent*) operating in constant-current mode with the tip immersed in the supernatant liquid. STM Tips were prepared by mechanically cutting a Pt/Ir wire

(80%/20%, diameter 0.2 mm). Prior to imaging, a drop of **AzoLC** solution was placed onto a freshly cleaved surface of highly oriented pyrolytic graphite (HOPG, grade ZYB, *Advanced Ceramics Inc.*, Cleveland, USA). The experiments were repeated in 2 – 3 sessions using different tips to check for reproducibility and to avoid experimental artifacts, if any. For analysis purposes, recording of a monolayer image was followed by imaging the graphite substrate underneath it under the same experimental conditions, except for increasing the current and lowering the bias. The images were corrected for drift through Scanning Probe Image Processor (SPIP) software (*Image Metrology ApS*), using the recorded graphite images for calibration purposes, allowing a more accurate unit cell determination. The unit cell parameters were determined by examining at least four images, and only the average values are reported. The images are *Gaussian* filtered. The imaging parameters are indicated in the figure caption: tunneling current (I_{set}), and sample bias (V_{bias}). The molecular models were built using HyperchemTM 7.0 program.

Preparation of Mixtures

Small Molecule Sample. **MeTBIB** was mixed with **AzoLC** in a 1:3 ratio in a 1:3 methanol/chloroform solvent mixture and the solvent was slowly removed from the sample by evaporation at 1 atm and at 21 °C. *Polymer Mixture*. **AzoLC** and polystyrene-block-poly(4-vinylpyridine)) were dissolved in chloroform and placed on a hot plate at 30 °C. After the solvent has evaporated (about 40 h) under ambient air conditions, the sample was annealed in a vacuum oven at 120 °C for 2 h and subsequently cooled to room temperature.

Synthetic Procedures

Ethyl 4-[(4-Hydroxyphenyl)diazenyl]benzoate (**1**). In a round-bottomed flask, 9.09 g of ethyl 4-aminobenzoate (1.0 equiv., 55.0 mmol) was dissolved in hydrochloric acid (1 M) and stirred at 0 °C. At this temperature, 3.80 g of sodium nitrite (1.0 equiv., 55.0 mmol), dissolved in 25 mL of water, was added dropwise to produce a diazonium salt solution. Meanwhile, 9.61 g of sodium carbonate (1.65 equiv., 90.8 mmol) and 5.81 g of phenol (1.0 equiv., 55.0 mmol) were dissolved in 100 mL of water at a temperature of 0 °C. The diazonium salt solution was added dropwise to this solution. The mixture was stirred for 3 h at 0 °C and then neutralized with hydrochloric acid (1 M). The product was filtered off, air-dried, and recrystallized in ethanol. Column chromatography (CH_2Cl_2), was performed to give ethyl 4-[(4-hydroxyphenyl)diazenyl]benzoate (**1**) in a yield of 66% (9.76 g, 36.1 mmol) as an orange solid. ^{1}H-NMR (400 MHz, $CDCl_3$, 300 K): 1.43 (*t*, ^3J = 7.1, CH_2*Me*); 4.41 (*q*, ^3J = 7.2, *C*H_2Me); 5.84 (br. *s*, OH); 6.97 (*d*, *J* = 8.2, 2 H, Ar-C-OH); 7.90 (*virt. dd*, ^3J = 8.5, ^3J = 8.1, 4 H, Ar-C-N); 8.18 (*d*, ^3J = 8.0, 2 H, Ar-C-COO). MALDI-TOF-MS: 271.27 ([*M* + H]$^+$, $C_{13}H_{10}N_2O_3^+$; calc. 270.10).

Ethyl 4-{[4-(Undec-10-en-1-yloxy)phenyl]diazenyl}-benzoate (**2**). A solution of 4.05 g of diazo compound **1** (15.0 mmol, 1.0 equiv.), 4.15 g of potassium carbonate (30.0 mmol, 2.0 equiv.), and 0.08 g of potassium iodide (0.49 mmol, 0.03 equiv.) was dissolved in 80 mL of acetone under argon. After 10 min of stirring, 1.06 mL of 10-bromoundec-1-ene (4.20 g, 18.0 mmol, 1.2 equiv.) was added drop-wise through syringe to the refluxing solution. The mixture was refluxed for 19 h and then cooled to room temperature. After adding 160 mL of water, the solution was extracted three times with 100 mL of dichloromethane, dried over magnesium sulfate, and filtered off. Column chromatography (pentane/diethylether 9:1) was performed to give 18% of ethyl ethyl 4-{[4-(undec-10-en-1-yloxy)phenyl]diazenyl}benzoate (**2**; 1.13 g, 2.67 mmol) as orange crystals. ^{1}H-NMR (400 MHz, $CDCl_3$, 300 K): 1.08 – 1.49 (*m*, 15 H, CH_2*Me*, $(CH_2)_6$); 1.82 (*quint.*-like, ^3J = 6.6, OCH_2*C*H_2); 2.05 (*q*, ^3J = 6.7, *C*H_2CH=CH_2); 4.05 (*t*, ^3J = 6.6, OCH_2); 4.41 (*q*, ^3J = 7.1, *C*H_2Me); 4.84 – 5.19 (*m*, CH=*C*H_2); 5.67 – 5.96 (*m*, *C*H=CH_2); 7.01 (*d*, ^3J = 9.0, 2 H, Ar-C-O); 7.92 (*dd*, ^3J = 9.0, ^3J = 8.5, 4 H, Ar-C-N); 8.17 (*d*, ^3J = 8.5, 2 H, Ar-C-COO).

Ethyl 4-[(4-{[11-(Pentadecamethylheptasiloxanyl)-undecyl]oxy}phenyl)diazenyl]benzoate (**3**). A flame-dried *Schlenk* flask was charged with 617 mg of diazo compound **2** (1.46 mmol, 1.0 equiv.), 834 mg of 1,1,1,3,3,5,5,7,7,9,9,11,11,13,13-pentadecamethylheptasiloxane (1.61 mmol, 1.1 equiv.) and one drop of *Karstedt*'s catalyst (2% Platinum(0)-1,3-divinyl-1,1,3,3-tetramethyldisiloxane complex solution in xylene) in 40 mL of dry dichloromethane under argon. The mixture was stirred at room temperature for 18 h under argon and then quenched with 40 mL of methanol. The solvents were removed under vacuum. Gradient column chromatography (heptane → dichloromethane) was performed to give 97% of ethyl 4-[(4-{[11-(pentadecamethylheptasiloxanyl)undecyl]oxy}phenyl)diazenyl]benzoate (**3**) (1.33 g, 1.41 mmol) as a dark red oil. ^{1}H-NMR (400 MHz, $CDCl_3$, 300 K): −0.22 to 0.39 (*m*, 45 H, $(SiMe_2)_6$, $SiMe_3$); 0.53 (*t*, ^3J = 7.2, $SiMe_2$–*C*H_2); 1.25 – 1.40 (*m*, 17 H, $(CH_2)_7$, CH_2*Me*); 1.43 (*t*, ^3J = 7.1, OCH_2CH_2*C*H_2); 1.82 (*quint.*-like, *J* = 6.5, OCH_2*C*H_2); 4.05 (*t*, ^3J = 6.5, OCH_2); 4.41 (*q*, ^3J = 7.1, 2 H, *C*H_2Me); 7.01 (*d*, ^3J = 8.9, 2 H, Ar-C-O); 7.92 (*dd*,

^3J = 8.9, ^3J = 8.3, 4 H, Ar-C-N); 8.17 (*d*, ^3J = 8.3, 2 H, Ar-C-COO). MALDI-TOF-MS: 941.44 ($[M + H]^+$, $C_{41}H_{80}N_2O_9Si_7^+$; calc. 940.42).

4-[(4-{[11-(Pentadecamethylheptasiloxanyl)undecyl]oxy}phenyl)diazenyl]benzoic Acid (**AzoLC**). A round-bottomed flask was charged with 724 mg of compound **3** (0.792 mmol, 1.0 equiv.), 1.43 g of trimethyltin hydroxide (7.95 mmol, 10.0 equiv.), and 5 mL of dichloromethane. The mixture was refluxed until completion (3 days), cooled to room temperature, and acidified to pH = 2 with phosphoric acid (0.5 N). The organic phase was washed with brine and dried over magnesium sulphate. Size exclusion chromatography (*Biobeads SX-3*, chloroform)) was performed to give 32% of 4-[(4-{[11-(pentadecamethylheptasiloxanyl)undecyl]oxy}phenyl)diazenyl]benzoic acid (**AzoLC**; 231 mg, 0.57 mmol) as an orange solid. IR (ATR): 2958*m* (C–H), 2917*m* (Me), 2848*m* (C–$H_{aromatic}$), 1683*s* (C=O), 1500*w* (N=N_{cis}), 1417*w* (N=N_{trans}), 1252*s* (Si–Me), 1027*s* (C–O), 839*m* (C–O), 795*s* (C–$H_{aromatic}$), 694*w* (Si–C). ^{1}H-NMR (400 MHz, $CDCl_3$, 300 K): −0.22 to 0.39 (*m*, 45 H, $(SiMe_2)_6$, $SiMe_3$); 0.53 (*t*, ^3J = 7.2, $SiMe_2$–CH_2); 1.25 – 1.40 (*m*, 14 H, $(CH_2)_7$); 1.43 (*t*, ^3J = 7.1, $OCH_2CH_2CH_2$), 1.83 (*quint.*-like, *J* = 6.5, OCH_2CH_2); 4.05 (*t*, ^3J = 6.5, OCH_2); 7.02 (*d*, ^3J = 9.1, 2 H, Ar-C-O); 7.94 (*dd*, ^3J = 8.6, ^3J = 6.7, 4 H, Ar-C-N); 8.25 (*d*, ^3J = 8.5, 2 H, Ar-C-COO). MALDI-TOF-MS: 913.40 ($[M + H]^+$, $C_{39}H_{76}N_2O_9Si_7^+$; calc. 913.64).

Supplementary Material

Supporting information for this article is available on the WWW under https://doi.org/10.1002/hlca.201800130.

Acknowledgements

The authors would like to acknowledge *Jody Lugger*, *Jeffrey Murphy*, *Dick Broer*, *Johan Lub*, *Bert Meijer*, *Sander Wuister*, and *Tamara Druzhinina* for many inspiring discussions, fruitful collaborations, and support. The authors thank *Bas de Waal* is for the synthesis of the ODMS molecule. The research in Eindhoven has been financially supported by the *Dutch Technology Foundation STW and ASML*. This work has also received funding from the Fund of *Scientific Research–Flanders (FWO)*, *KU Leuven*, and *ERC* Grant Agreement No. 340324. *G. M.* acknowledges a *Marie Skłodowska-Curie Individual Fellowship*.

Author Contribution Statement

K. N. and *A. S.* conceived and designed the experiments and wrote the paper. *D. H.* performed the synthesis. *K. N.* and *S. J.* performed the characterization. *G. V.*, *J. T.*, and *S. F.* contributed the STM analysis.

References

[1] K. Nickmans, A. P. H. J. Schenning, 'Directed Self-Assembly of Liquid-Crystalline Molecular Building Blocks for Sub-5 Nm Nanopatterning', *Adv. Mater.* **2018**, *30*, 1703713.
[2] H.-C. Kim, S.-M. Park, W. D. Hinsberg, 'Block Copolymer Based Nanostructures: Materials, Processes, and Applications to Electronics', *Chem. Rev.* **2010**, *110*, 146 – 177.
[3] J. Lugger, D. J. Mulder, R. Sijbesma, A. Schenning, 'Nanoporous Polymers Based on Liquid Crystals', *Materials* **2018**, *11*, 104.
[4] J. N. L. Albert, T. H. Epps III, 'Self-Assembly of Block Copolymer Thin Films', *Materials Today* **2010**, *13*, 24 – 33.
[5] C. M. Bates, F. S. Bates, '50th Anniversary Perspective: Block Polymers–Pure Potential', *Macromolecules* **2017**, *50*, 3 – 22.
[6] C. Sinturel, F. S. Bates, M. A. Hillmyer, 'High χ–Low *N* Block Polymers: How Far Can We Go?', *ACS Macro Lett.* **2015**, *4*, 1044 – 1050.
[7] A. P. H. J. Schenning, Y. C. Gonzalez-Lemus, I. K. Shishmanova, D. J. Broer, 'Nanoporous Membranes Based on Liquid Crystalline Polymers', *Liq. Cryst.* **2011**, *38*, 1627 – 1639.
[8] A. Schenning, G. P. Crawford, D. J. Broer, 'Liquid Crystal Sensors', CRC Press, Taylor & Francis Group, Boca Raton, 2018.
[9] D. J. Mulder, A. P. H. J. Schenning, C. W. M. Bastiaansen, 'Chiral-Nematic Liquid Crystals as One Dimensional Photonic Materials in Optical Sensors', *J. Mater. Chem. C* **2014**, *2*, 6695 – 6705.
[10] D. J. Broer, C. W. M. Bastiaansen, M. G. Debije, A. P. H. J. Schenning, 'Functional Organic Materials Based on Polymerized Liquid-Crystal Monomers: Supramolecular Hydrogen-Bonded Systems', *Angew. Chem. Int. Ed.* **2012**, *51*, 7102 – 7109.
[11] D. L. Gin, R. D. Noble, 'Designing the Next Generation of Chemical Separation Membranes', *Science* **2011**, *332*, 674 – 676.
[12] D. L. Gin, J. E. Bara, R. D. Noble, B. J. Elliott, 'Polymerized Lyotropic Liquid Crystal Assemblies for Membrane Applications', *Macromol. Rapid Commun.* **2008**, *29*, 367 – 389.
[13] M. O'Neill, S. M. Kelly, 'Liquid Crystals for Organic Field-Effect Transistors', in 'Liquid Crystalline Semiconductors', Eds. R. J. Bushby, S. M. Kelly, M. O'Neill, Springer Netherlands, 2013, pp. 247 – 268.
[14] M. Kumar, S. Kumar, 'Liquid Crystals in Photovoltaics: A New Generation of Organic Photovoltaics', *Polym. J.* **2017**, *49*, 85 – 111.
[15] C. Tschierske, 'Development of Structural Complexity by Liquid-Crystal Self-Assembly', *Angew. Chem. Int. Ed.* **2013**, *52*, 8828 – 8878.
[16] H. K. Bisoyi, Q. Li, 'Light-Driven Liquid Crystalline Materials: From Photo-Induced Phase Transitions and Property Modulations to Applications', *Chem. Rev.* **2016**, *116*, 15089 – 15166.
[17] K. Nickmans, G. M. Bögels, C. Sánchez-Somolinos, J. N. Murphy, P. Leclère, I. K. Voets, A. P. H. J. Schenning, '3D Orientational Control in Self-Assembled Thin Films with Sub-5 nm Features by Light', *Small* **2017**, *13*, 1701043.
[18] H. Hu, M. Gopinadhan, C. O. Osuji, 'Directed Self-Assembly of Block Copolymers: A Tutorial Review of Strategies for

Enabling Nanotechnology with Soft Matter', *Soft Matter* **2014**, *10*, 3867 – 3889.
[19] E. L. Heeley, D. J. Hughes, Y. El Aziz, I. Williamson, P. G. Taylor, A. R. Bassindale, 'Properties and Self-Assembled Packing Morphology of Long Alkyl-Chained Substituted Polyhedral Oligomeric Silsesquioxanes (POSS) Cages', *Phys. Chem. Chem. Phys.* **2013**, *15*, 5518 – 5529.
[20] N. Kim, D.-Y. Kim, M. Park, Y.-J. Choi, S. Kim, S. H. Lee, K.-U. Jeong, 'Asymmetric Organic-Inorganic Hybrid Giant Molecule: Hierarchical Smectic Phase Induced from POSS Nanoparticles by Addition of Nematic Liquid Crystals', *J. Phys. Chem. C* **2015**, *119*, 766 – 774.
[21] K. Nickmans, J. N. Murphy, B. de Waal, P. Leclère, J. Doise, R. Gronheid, D. J. Broer, A. P. H. J. Schenning, 'Sub-5 nm Patterning by Directed Self-Assembly of Oligo(Dimethylsiloxane) Liquid Crystal Thin Films', *Adv. Mater.* **2016**, *28*, 10068 – 10072.
[22] K. Nickmans, P. Leclère, J. Lub, D. J. Broer, A. P. H. J. Schenning, 'Reactive Oligo(Dimethylsiloxane) Mesogens and Their Nanostructured Thin Films', *Soft Matter* **2017**, *13*, 4357 – 4362.
[23] K. Nickmans, R. C. P. Verpaalen, J. N. Murphy, A. P. H. J. Schenning, 'Sub-5 nm Structured Films by Hydrogen Bonded Siloxane Liquid Crystals and Block Copolymers', *J. Mater. Chem. C* **2018**, *6*, 3042 – 3046.
[24] J. A. Berrocal, R. H. Zha, B. F. M. de Waal, J. A. M. Lugger, M. Lutz, E. W. Meijer, 'Unraveling the Driving Forces in the Self-Assembly of Monodisperse Naphthalenediimide-Oligodimethylsiloxane Block Molecules', *ACS Nano* **2017**, *11*, 3733 – 3741.
[25] M. García-Iglesias, B. F. M. de Waal, I. de Feijter, A. R. A. Palmans, E. W. Meijer, 'Nanopatterned Superlattices in Self-Assembled C_2-Symmetric Oligodimethylsiloxane-Based Benzene-1,3,5-Tricarboxamides', *Chem. Eur. J.* **2015**, *21*, 377 – 385.
[26] C. Tschierske, 'Micro-Segregation, Molecular Shape and Molecular Topology-Partners for the Design of Liquid Crystalline Materials with Complex Mesophase Morphologies', *J. Mater. Chem.* **2001**, *11*, 2647 – 2671.
[27] B. van Genabeek, B. F. M. de Waal, M. M. J. Gosens, L. M. Pitet, A. R. A. Palmans, E. W. Meijer, 'Synthesis and Self-Assembly of Discrete Dimethylsiloxane-Lactic Acid Diblock Co-Oligomers: The Dononacontamer and Its Shorter Homologues', *J. Am. Chem. Soc.* **2016**, *138*, 4210 – 4218.
[28] K. C. Nicolaou, A. A. Estrada, M. Zak, S. H. Lee, B. S. Safina, 'A Mild and Selective Method for the Hydrolysis of Esters with Trimethyltin Hydroxide', *Angew. Chem. Int. Ed.* **2005**, *44*, 1378 – 1382.
[29] S. De Feyter, F. C. De Schryver, 'Self-Assembly at the Liquid/Solid Interface: STM Reveals', *J. Phys. Chem. B* **2005**, *109*, 4290 – 4302.
[30] A. Ciesielski, C.-A. Palma, M. Bonini, P. Samorì, 'Towards Supramolecular Engineering of Functional Nanomaterials: Pre-Programming Multi-Component 2D Self-Assembly at Solid-Liquid Interfaces', *Adv. Mater.* **2010**, *22*, 3506 – 3520.
[31] K. S. Mali, K. Lava, K. Binnemans, S. De Feyter, 'Hydrogen Bonding Versus van der Waals Interactions: Competitive Influence of Noncovalent Interactions on 2D Self-Assembly at the Liquid-Solid Interface', *Chem. Eur. J.* **2010**, *16*, 14447 – 14458.
[32] X. Miao, Z. Cheng, B. Ren, W. Deng, 'Hydrogen Bonds Induced Supramolecular Self-Assembly of Azobenzene Derivatives on the Highly Oriented Pyrolytic Graphite Surface', *Surf. Sci.* **2012**, *606*, L59 – L63.
[33] J. A. Berrocal, J. Teyssandier, O. J. G. M. Goor, S. De Feyter, E. W. Meijer, 'Supramolecular Loop Stitches of Discrete Block Molecules on Graphite: Tunable Hydrophobicity by Naphthalenediimide End-Capped Oligodimethylsiloxane', *Chem. Mater.* **2018**, *30*, 3372 – 3378.
[34] J. A. M. Lugger, R. P. Sijbesma, 'Easily Accessible Thermotropic Hydrogen-Bonded Columnar Discotic Liquid Crystals from Fatty Acid–Tris-Benzoimidazolyl Benzene Complexes', *ChemistryOpen* **2016**, *5*, 580 – 585.
[35] G. ten Brinke, J. Ruokolainen, O. Ikkala, 'Supramolecular Materials Based On Hydrogen-Bonded Polymers', in 'Hydrogen Bonded Polymers', Vol. 207, Ed. W. Binder, Springer, Berlin, Heidelberg, 2007, pp. 113 – 177.
[36] A. H. Hofman, M. Reza, J. Ruokolainen, G. ten Brinke, K. Loos, 'Hierarchical Self-Assembly of Symmetric Supramolecular Double-Comb Diblock Copolymers: A Comb Density Study', *Macromolecules* **2014**, *47*, 5913 – 5925.
[37] O. Ikkala, G. ten Brinke, 'Functional Materials Based on Self-Assembly of Polymeric Supramolecules', *Science* **2002**, *295*, 2407 – 2409.

Received July 13, 2018
Accepted August 2, 2018